Landslides (2019) 16:1965–1979
DOI 10.1007/s10346-019-01247-y
Received: 12 March 2019
Accepted: 22 July 2019
Published online: 1 August 2019
© Springer-Verlag GmbH Germany
part of Springer Nature 2019

Limin Zhang · Te Xiao · Jian He · Chen Chen

Erosion-based analysis of breaching of Baige landslide dams on the Jinsha River, China, in 2018

Abstract The Yangtze River is one of the most important rivers in China due to its large basin size, the large population along the river, and the numerous large dams and reservoirs on the river. The Jinsha River, the upper reach of the Yangtze River, was dammed twice recently at Baige, Tibet, one on 10 October 2018 and the other on 3 November 2018 (UTC + 8). Accordingly, two large landslide dams, 61 m and 96 m in height to the lowest dam crest, were formed in a 3-week interval. Due to the large inflow rates at the time of damming, the barrier lake level rose rapidly, posing huge risks to the downstream residents and properties. In managing the landslide dam risk, one of the important tasks is to predict the dam breaching flood beforehand. This paper focuses on rapid prediction of the dam breaching hydrograph and breach geometric parameters of the two landslide dams. The predictions were made timely before the breaching of the two landslide dams using both erosion-based empirical equations and numerical simulation and were refined based on detailed field investigation at the site after breaching. Comprehensive field investigations were conducted to determine the geological structures of the landslide dams, characterize the erodibility of dam materials, and measure the final beach dimensions. The simulated dam breaching processes, outflow hydrographs, lake water level changes, and final breach dimensions were validated by field observations. Compared with the hypothetical scenario without a diversion channel on the second landslide dam, a diversion channel 15 m in depth successfully lowered the peak flood discharge by about one third and helped to mitigate the flood risk significantly. The analysis outcome serves as basis for warning and evacuation of the downstream residents and making appropriate engineering risk mitigation plans.

Keywords Landslide · Landslide dam · Dam breaching · Yangtze River · Erosion · Flood

Formation and beaching of two landslide dams

The Jinsha River (Fig. 1a) is the upper course of the Yangtze River, the longest river in China and the third longest river in the world. It originates from Qinghai Province and flows through Tibet, Sichuan and Yunnan Provinces. The Jinsha River is 2290 km long, with a basin area of approximately 340,000 km^2 and an elevation drop of approximately 3250 m. The annual average flow rate is about 4500 m^3/s. Given the rich hydropower resources, more than 25 large dams have been completed, under construction or planned along the Jinsha River for power generation and flood control.

In 2018, the Jinsha River was dammed twice, one on 10 October and the other on 3 November (Beijing time, UTC + 8 throughout the paper). At 22:06 on 10 October, a large landslide occurred at Baige, Tibet (98°42′17.98″ E 31°4′56.41″ N, Fig. 1b), on the upper reach of the Jinsha River. The landslide scar was located at the right bank of the river at an elevation of approximately 3700 m, and the landslide front blocked the river with an internal relief of over 800 m and a travel distance of 1500 m. The total volume of the landslide was about 25×10^6 m^3, the majority of which formed a landslide dam (Fig. 2a) 61 m in height to the lowest crest and about 1500 m in length along the river. This was the first time in the recent history that the Yangtze River was completely blocked. The lake water level rose rapidly as the incoming flow rate was as large as 1680 m^3/s. The landslide dam was naturally overtopped at 17:30, 12 October, and breached in about 21 h (Fig. 2b). The river resumed its base flow at the dam site at 14:30 on 13 October. The life span of the landslide dam was 2.7 days. The dam breaching flow, peaked at about 10,000 m^3/s, marched along the river, posing huge risks on the downstream hydropower projects and residents. The upstream cofferdam for a high rockfill dam at Suwalong (Fig. 1a) was nearly overtopped.

About 3 weeks after the successful disposal of the landslide dam formed on 10 October, a second slide occurred at the same site at 17:15, 3 November, with additional source and entrainment volumes of about 3×10^6 m^3 and 8×10^6 m^3, respectively (Fig. 3a). The landslide debris deposited on the breach formed earlier, forming a new dam 96 m in height to the lowest crest and about 1000 m in length along the river and blocking the Jinsha River once again. With an incoming flow rate of about 800 m^3/s, the lake volume increased gradually. When full, the lake volume would reach 750×10^6 m^3, posing much greater risks than the lake that breached on 12 October. To mitigate the risks, a diversion channel, 220 m in length, 15 m in depth, 42 m in top width and 3 m in bottom width was excavated in 3 days (Fig. 3b), which decreased the lake capacity significantly to 500×10^6 m^3. Finally, the dam was overtopped at 04:45, 12 November, and the breaching process lasted over 50 h (Fig. 3c, d). The peak dam breaching flow rate reached 33,900 m^3/s. The flow rate at the dam site reverted to the base flow at 08:00 on 14 November, indicating a lifespan of the landslide dam of 10.6 days. Meanwhile, the dam breaching flood marched over 670 km before it was captured in Liyuan Reservoir (Fig. 1a) and five other large reservoirs on the Jinsha River. During the 2-day flood marching process, many bridges over the river such as Zhubalong Bridge (Figs. 1a and 4a) were destroyed, the National Highway G318 was temporally suspended, and numerous towns were flooded. The cofferdams of Suwalong Dam (Figs. 1a and 4b) were removed before the arrival of the flood to prevent amplification of flood by cascading failures of the landslide dam and the cofferdams.

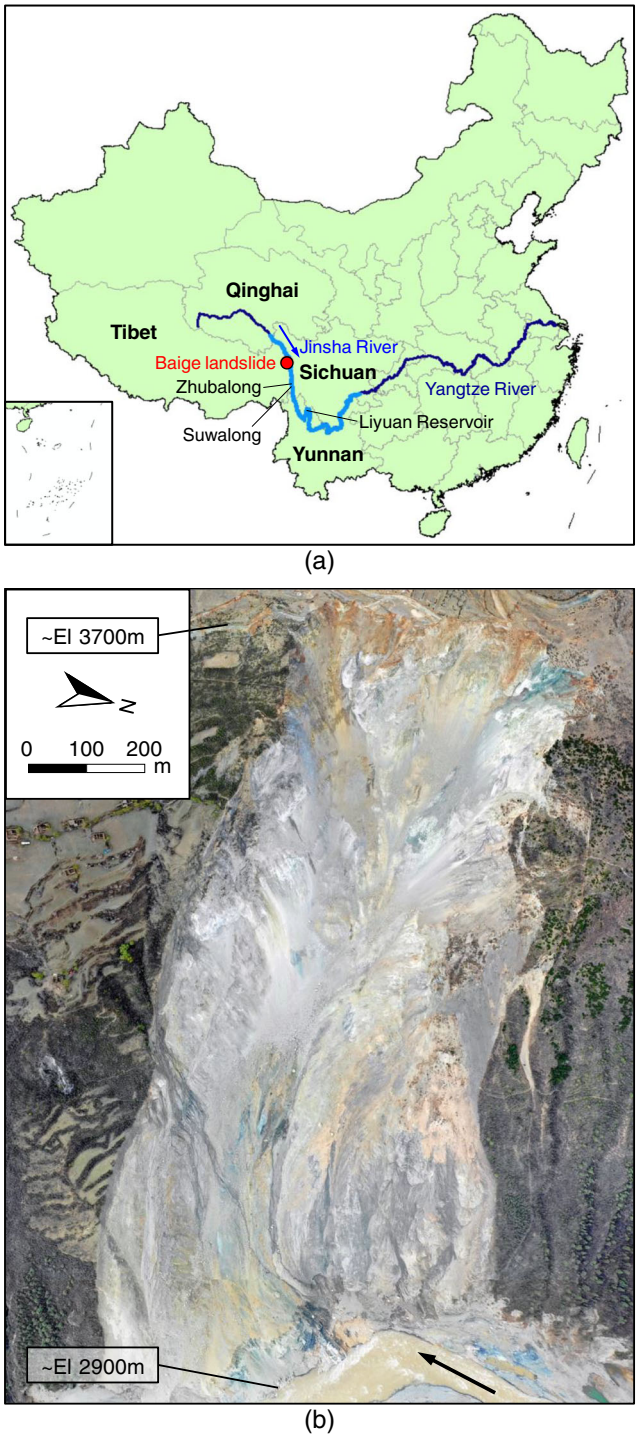

Fig. 1 Baige landslides: **a** location; **b** top view (photo credit: Zhang LM)

When landslide dams form on a major river, such as the two dams on the Jinsha River, many urgent technical issues arise in managing their risks:

(1) Detailed study of causes and process of the landslides, as well as possibility of reactivation of new landslides in short term through field investigations and remote sensing techniques (e.g., Chang et al. 2011; Dong et al. 2014; Fan et al. 2019);
(2) Hydrologic monitoring in the river basin and forecast of near future inflow into the barrier lake (e.g., Cai et al. 2019);
(3) Prediction of dam breaching parameters, including the breach geometry and the outflow hydrograph (e.g., Peng and Zhang 2012a; Chen et al. 2015; Chen et al. 2018);
(4) Analysis of dam breaching flood routing downstream the dam and assessment of the flood risks (e.g., Cui et al. 2012; Peng and Zhang 2012b, 2012c);
(5) Development of structural or non-structural measures to mitigate the risks (e.g., Cui et al. 2012; Peng and Zhang 2013a, 2013b; Chen et al. 2015; Shi et al. 2017; Chen et al. 2018).

This paper focuses on rapid prediction of the dam breaching hydrograph and breach geometric parameters of the two landslide dams on the Jinsha River in 2018. Detailed field investigations were conducted and the breaching parameters were computed using both erosion-based empirical equations and numerical simulation. In this paper, the geological structures of the two landslide dams, the theoretical basis of dam breaching simulation, and the determination of soil erodibility parameters are introduced. The detailed breaching processes and the resulting outflow hydrographs are presented. The causes and dynamics of the landslides have been explored by Fan et al. (2019), Ouyang et al. (2019), and Zhang et al. (2019) and are beyond the scope of this paper.

Geological conditions

The landslide site is located in the north of the Hengduan Mountains. According to geological surveys (TARGS 1992), approximately 80% of the area has elevations between 4000 and 5000 m; less than 1% of the area is below elevation 3000 m, primarily along the valleys of the Jinsha River and the Lancang River. The area has a continental cold weather condition, with average annual temperatures of 0 °C above 4000 m and 3.2–7.0 °C below 3500 m. The annual rainfall is approximately 500 mm, mostly in June–September. The snow season spans approximately 6 months, from October to April.

Moderate vegetation is found in the landslide area (Fig. 1b). The gradient at the landslide scar is approximately 20–40°. As shown in the geology map (Fig. 5) (TARGS 1992), the primary bedrocks at the site are plagioclase gneiss ($P_t xn^a$) and serpentinite ($\phi\omega_4$). Several faults develop along the northwestern direction. A tension zone had been observed in the shattered rock mass after experiencing a long period of downward movements, and both the landslides on 10 October and 3 November were the outcome of the long-term slope deformations (Fan et al. 2019).

Based on geometrical and geological information from field surveys, representative cross sections of the two dams are generated, as shown in Fig. 6. The longitudinal section is cut along the diversion channel for the second dam, above

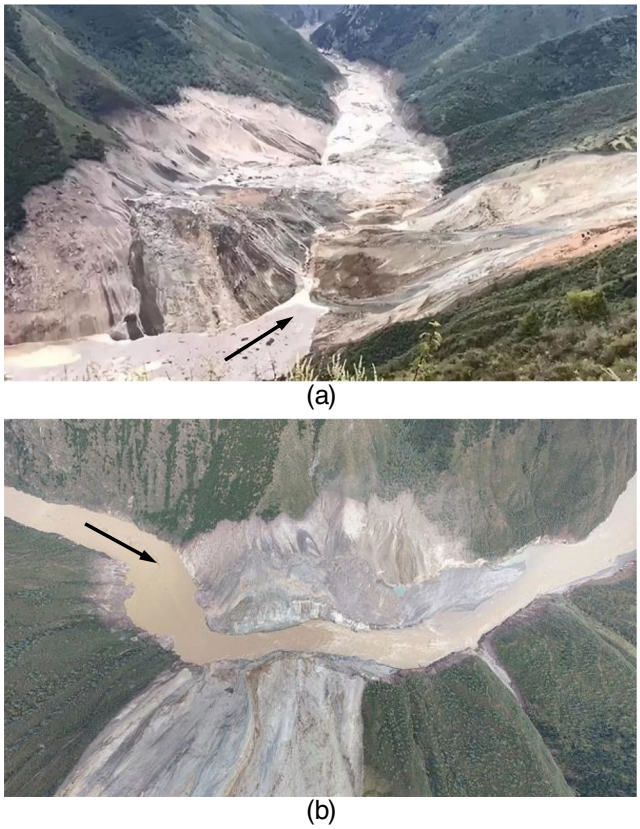

Fig. 2 First Baige landslide dam: **a** formation; **b** after breaching (photo credit: **a** CCTV.com; **b** Changjiang Water Resources Committee)

which the dam would be overtopped, and represents the most dangerous profiles associated with the lowest crest elevations and the shortest overflow paths. The elevation of the riverbed is about 2870 m and the lowest crest elevations of the two landslide dams are 2931 and 2966 m, respectively, defining effective dam heights of 61 and 96 m, respectively, for the dam breaching analysis to be reported later. As the diversion channel is excavated at the lowest crest of the second landslide dam, its bottom elevation is 2951 m.

Hydrologic conditions

Utilizing a digital elevation model AW3D30 (Tadono et al. 2014), released by the Japan Aerospace Exploration Agency with horizontal resolution of 30 m and height accuracy of 5 m, the barrier lakes (i.e., inundation areas) at elevations 2931, 2951 and 2966 m are determined as shown in Fig. 7a. The lakes stretch 48, 64 and 72 km upstream the dam, respectively, and the inundation areas are 9.6, 15.1 and 20.1 km^2, respectively, at these three lake water levels. Indeed, several settlement areas such as Boluo Village and Jinsha Village, 20 and 58 km upstream the dam, respectively, were inundated. Figure 7b presents the relation between barrier lake capacity and lake surface elevation derived from the digital elevation model. The lake volumes are measured as 249×10^6, 494×10^6, 757×10^6 m^3, respectively, at the three critical water levels.

The incoming flow rate into the first barrier lake on 12 October, measured at the upstream hydrological station, was 1680 m^3/s, while the outflow rate seeping through the dam was 100 m^3/s. Hence, the time required to fill the first barrier lake was only 1.8 days, meaning that the lake would be short lived. The second landslide dam was much higher than the first dam and the capacity of the barrier lake was tripled, posing much greater risks to the

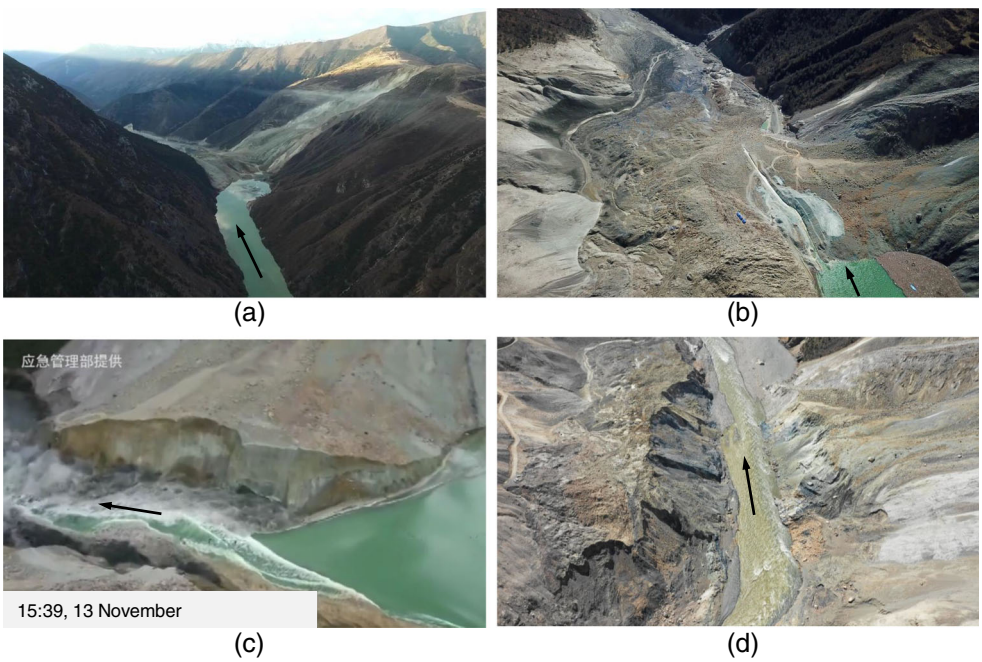

Fig. 3 Second Baige landslide dam: **a** formation; **b** diversion channel; **c** during breaching; **d** after breaching (photo credit: **a** CCTV.com; **b** Red Star News; **c** Ministry of Emergency Management of China; **d** Zhang LM)

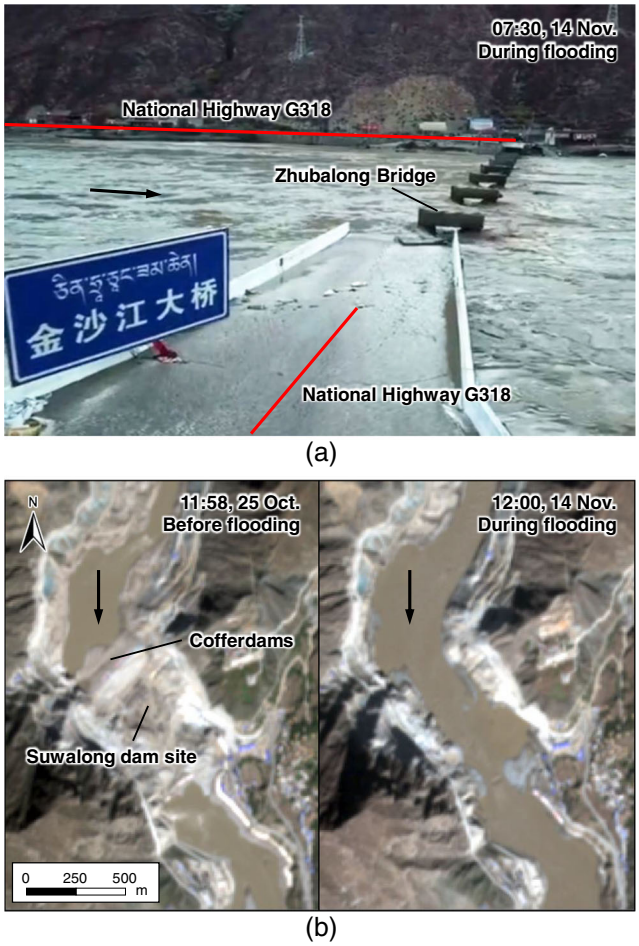

Fig. 4 Damages induced by second breaching of Baige landslide dam: **a** Zhubalong Bridge (photo credit: xinhuanet.com); **b** cofferdams of Suwalong dam (source: Sentinel-2)

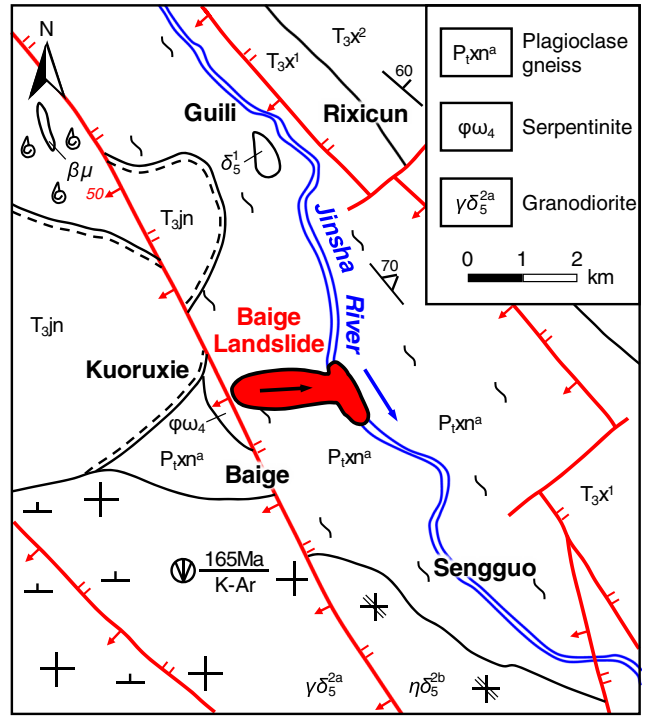

Fig. 5 Geological condition in the landslide region

elements downstream the dam. On 3 November, the incoming flow rate into the second barrier lake was measured as about 800 m^3/s, which had decreased significantly compared with that in mid-October and would fill the lake in 12 days. To mitigate the risks, it was decided to excavate a 15-m-deep diversion channel across the dam to decrease the weir elevation and the lake volume. As a result, the time to fill the lake was reduced to about 8 days. How the diversion channel helps to reduce the dam breaching flow rate will be analyzed later in this paper.

Erodibility of dam materials

The failure modes of landslide dams have been examined based on past case histories (Costa and Schuster 1988; Peng and Zhang 2012a; Danka and Zhang 2015; Zhang et al. 2016). According to Peng and Zhang (2012a), approximately 91% of landslide dams failed by overtopping due to the lack of flood-passing facilities; 8% failed by piping erosion because of the small hydraulic gradient related to the gentle dam slopes; and only in rare cases (1%) did a landslide dam fail by slope instability, again due to its gentle slopes. Further dam failure statistics show that most landslide dams were short lived, with 71%, 51% and 34% of landslide dams breached within 1 month, 1 week, and 1 day, respectively (Peng and Zhang 2012a). Indeed, both the dams formed on the Jinsha River in October and November 2018 failed due to overtopping, with life spans of 2.7 and 10.6 days, respectively.

As overtopping is the dominant failure mode of landslide dams, the most critical parameter that governs the overtopping erosion process is the erodibility of dam materials. Erodibility may be measured in a quantitative or qualitative manner. Hanson and Simon (2001) express the erosion rate E as a linear function of the erosive stress induced by flowing water as:

$$E = K_d(\tau - \tau_c) \tag{1}$$

where τ = shear stress at the soil/water interface and is related to hydraulic radius and energy slope; K_d = coefficient of erodibility; and τ_c = critical shear stress at initiation of soil erosion. A higher value of K_d and a smaller value of τ_c correspond to a higher soil erodibility. Nonlinear variations of Eq. (1) are available in the literature (e.g., Chen et al. 2018). In practice, K_d and τ_c can be determined in the field or in the laboratory using flume tests, submerged jet-index tests, the erosion function apparatus, cylindrical erosion tests, or other test methods (e.g., Hanson and Simon 2001; Briaud 2008; Chang et al. 2011; Chen et al. 2018; Zhu and Zhang 2016). Zhang et al. (2016) presented a detailed review of the methods for determining the erodibility of soil materials. Empirical equations are also available to estimate the erodibility parameters as (e.g., Annandale 2006; Chang et al. 2011)

$$K_d = 20075e^{4.77}C_u^{-0.76} \tag{2}$$

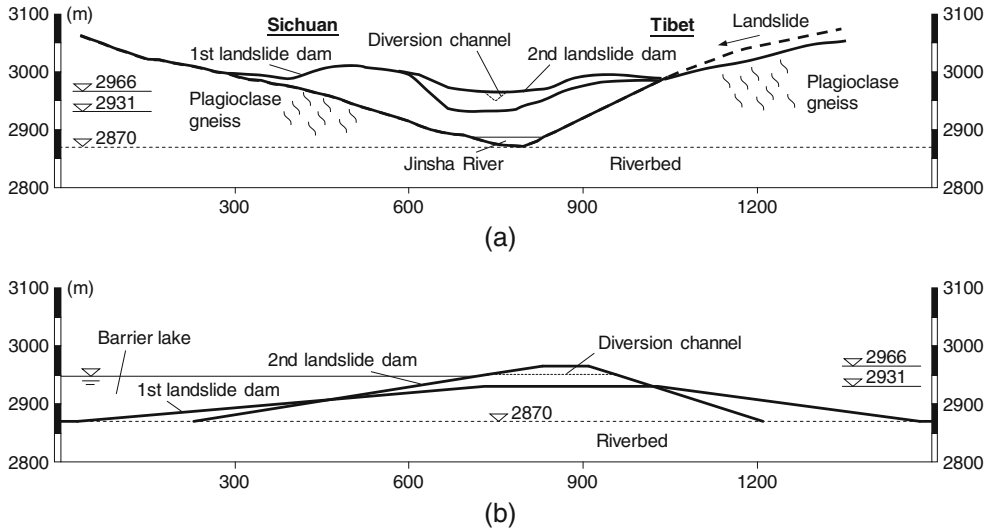

Fig. 6 Cross sections of Baige landslide dams: **a** across the river; **b** along the river

$$\tau_c = \begin{cases} 6.8(PI)^{1.68}(FC)^{-1.73}e^{-0.97}, & \text{for } FC > 10\% \\ \frac{2}{3}gd_{50}(\rho_s - \rho_w)\tan\phi, & \text{for } FC \leq 10\% \end{cases} \quad (3)$$

where e = void ratio; C_u = coefficient of uniformity; PI = plasticity index; FC = fines content; d_{50} = median particle size; ρ_s = mass density of soil; ρ_w = mass density of water; and ϕ = friction angle. Based on values of K_d and τ_c or values of erosion rate and flow velocity, the erodibility can be classified into multiple grades qualitatively, namely very high, high, medium, low, and very low erodibility (e.g., Briaud 2008).

Representative materials of the Baige landslide dam are shown in Fig. 8a. The upper soil layers are loose gravelly sand (P2 in Fig. 8a) while the bottom and the majority of the dam body consist of weathered plagioclase gneiss (P1 and P3 in Fig. 8a). The plagioclase in the gneiss is prone to decomposition so that the rock is extremely weak and can be broken by hand. Figure 9 shows the grain size distributions of samples from various elevations on the dam, as well as the values of dry density and void ratio. The shallow soils at elevations 2940–2970 m are rather loose, with dry density values of 1469–1591 kg/m^3 and void ratio values of 0.70–0.84. The weathered plagioclase gneiss (sampling points L2–1, L3–1, and L4–1), on the other hand, is relatively dense with dry density values of 1831–2062 kg/m^3 and void ratio values of 0.31–0.48. Taking the samples from L2–2 (A), L3–1 (B), and L1–1 (C) (i.e., three bold curves in Fig. 9a) as indicative materials, the values of K_d and τ_c along depth can be calculated using Eqs. (2) and (3) and plotted in Fig. 10 as "Baige (field)" points. For comparison, the distributions of K_d and τ_c with elevation for the upper part of the Tangjiashan landslide dam (Peng et al. 2014) are transplanted to the Baige landslide dams with slight adjustments on the depth as shown in Fig. 10. The second Baige landslide dam has a slightly higher erodibility than the first dam because it involves a residual landslide of finer materials.

The erodibility of the Baige landslide dams was also benchmarked against that of the Donghekou, Libaisi, and Tangjiashan landslide dams in 2008, and that of the Yigong landslide dam in 2000. Zhang et al. (2011) and Chang et al. (2011) conducted field investigations on landslide particle flow characteristics and landslide dam erodibility at Donghekou, Libaisi, and Tangjiashan. The erodibility of the fully disintegrated landslide deposits at the three sites were rated "medium", except for the very loose and relatively fine soil cover on the surface, which was rated "medium-high". All the three landslides at Donghekou, Libaisi, and Tangjiashan initiated as rock slides. As the rock mass detached off the scar and marched down the slope, rock mass disintegration, particle crushing and reverse segregation occurred. Hence the original rock mass evolved into smaller pieces and further to coarse or fine grained soils after a long travel distance. The travel distance of the Donghekou slide was more than 2000 m, and the materials in the deposition zone were loose or medium dense sandy gravel or gravelly sand with dry density values of 1237–1485 kg/m^3 (Chang et al. 2011; Zhang et al. 2011). The Tangjiashan landslide involved a shorter travel distance of about 380 m (Cui et al. 2012). The rock mass did not fully disintegrate and the bottom part of the barrier dam still consisted of rock mass layers, as shown in Fig. 8b. Hence, the upper part of the soil was of medium erodibility whereas the bottom rock mass was of very low erodibility. The Yigong landslide is another typical example of a long distance landslide. The landslide scar was located at an elevation of approximately 5000 m and the landslide debris marched over 8 km into the Yigong River (Zhou et al. 2016). After such a long-distance travel, the material at the dam site became silty sand, which falls into the "high" erodibility category.

The first landslide dam debris at Baige was subject to a travel distance of approximately 1500 m and the material was considered fully disintegrated (Figs. 2a and 8a). The material layering is similar to the upper part of the Tangjiashan landslide dam, hence rated "medium" erodibility. The second slide occurred at the margins of the scar of the first slide, with strong entrainment of the material of the first landslide along the flow path. The new

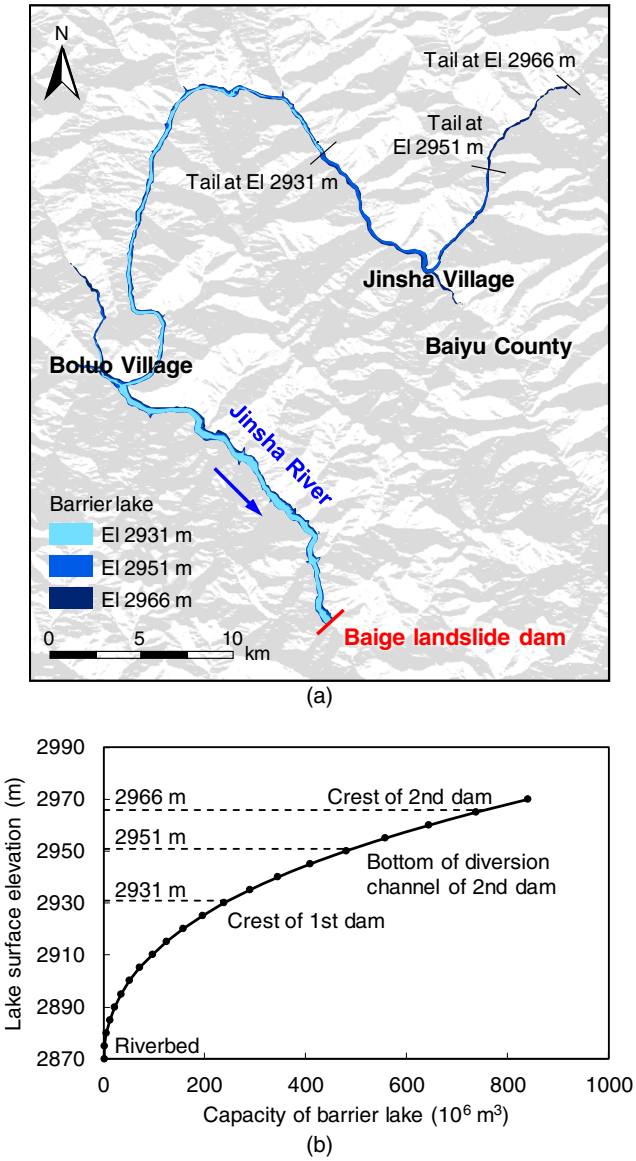

Fig. 7 Barrier lakes at different elevations: **a** inundation areas; **b** lake capacity-elevation curve

barrier deposit formed in the second slide was finer and looser than that in the first landslide. Hence, its erodibility is rated "medium-high".

Empirical analysis of dam breaching parameters

As 34% of the past landslide dams lasted only 1 day and 51% within 1 week, detailed site investigations within such a short period are not likely, particularly for those without road access. Consequently, empirical equations are often applied to enable rapid assessment of breach parameters and flood risks.

Various empirical equations have been proposed to estimate the peak flow rate (Costa 1985; Costa and Schuster 1988; Walder and O'Connor 1997; Peng and Zhang 2012a), breach development duration, and breach size (Peng and Zhang 2012a) with a few basic parameters such as dam height, lake volume, and erodibility of dam material. The grade of soil erodibility serves as an important parameter in those proposed by Peng and Zhang (2012a). It should be cautioned that empirical models for manmade earth and rockfill dams cannot be applied to landslide dams. Otherwise, the peak outflow rate could be overestimated by 200% and the breaching duration underestimated by 50% (Peng and Zhang 2012a).

Given the evaluated erodibility in the previous section (i.e., "medium" erodibility for the first dam and "medium-high" erodibility for the second dam) and basic parameters of the dam and lake in Table 1, the peak discharge, breaching duration, and breach size are estimated using empirical equations, as summarized in Table 2. Note that the results of the "medium-high" case are obtained by taking the average of the results from "high" erodibility and "medium" erodibility cases. Compared with the observed peak flow rates (i.e., 10,000 and 33,900 m^3/s), the equations proposed by Peng and Zhang (2012a) offer reasonable predictions, namely 7995 and 30,515 m^3/s for the two Baige landslide dams, respectively. In addition, those equations also give comparable estimates of the breach size. The breach depth and breach bottom width are relatively accurate while the breach top width is underestimated using the empirical equation. This is mainly due to the large elevation difference between the lowest and topmost dam crests (Fig. 6a). While the calculated breach top width is in reference to the lowest dam crest, the observed one is in reference to the topmost crest. The collapse of breach walls above the lowest dam crest on both sides of the river enlarges the breach top width significantly.

Physically based simulation of dam breaching process

Erosion-based dam breaching model

Different to empirical analysis, physically based simulation is able to produce the entire breaching process. An erosion-based numerical model, DABA (Chang and Zhang 2010; Zhang et al. 2016), is used in this study to rapidly simulate the entire dam breaching process. In this model, the dam breaches as the overtopping water flow erodes the dam materials. The bed and bank erosion rates are calculated using Eq. (1) and the flow rate through the breach is calculated using a broad-crested weir flow equation (e.g., Singh and Scarlatos 1988). More detailed formulations can be referred to Chang and Zhang (2010) and Zhang et al. (2016).

Figure 11 shows the breaching process of a landslide dam in DABA, which is divided into two phases, namely the breach initiation phase and the breach development phase, signaled by a significant increase in the flow rate. The breach evolution on the cross and longitudinal sections experiences three erosion stages:

(1) Stage I. On the longitudinal section (i.e., stage L-I), the water flow cuts the toe of the downstream slope until it reaches a limit angle β_f, and the breach bottom is only eroded slightly. On the cross section (i.e., stage C-I), the breach top width does not change, but the breach depth, bottom width, and bank slope increase gradually until the bank slope reaches a

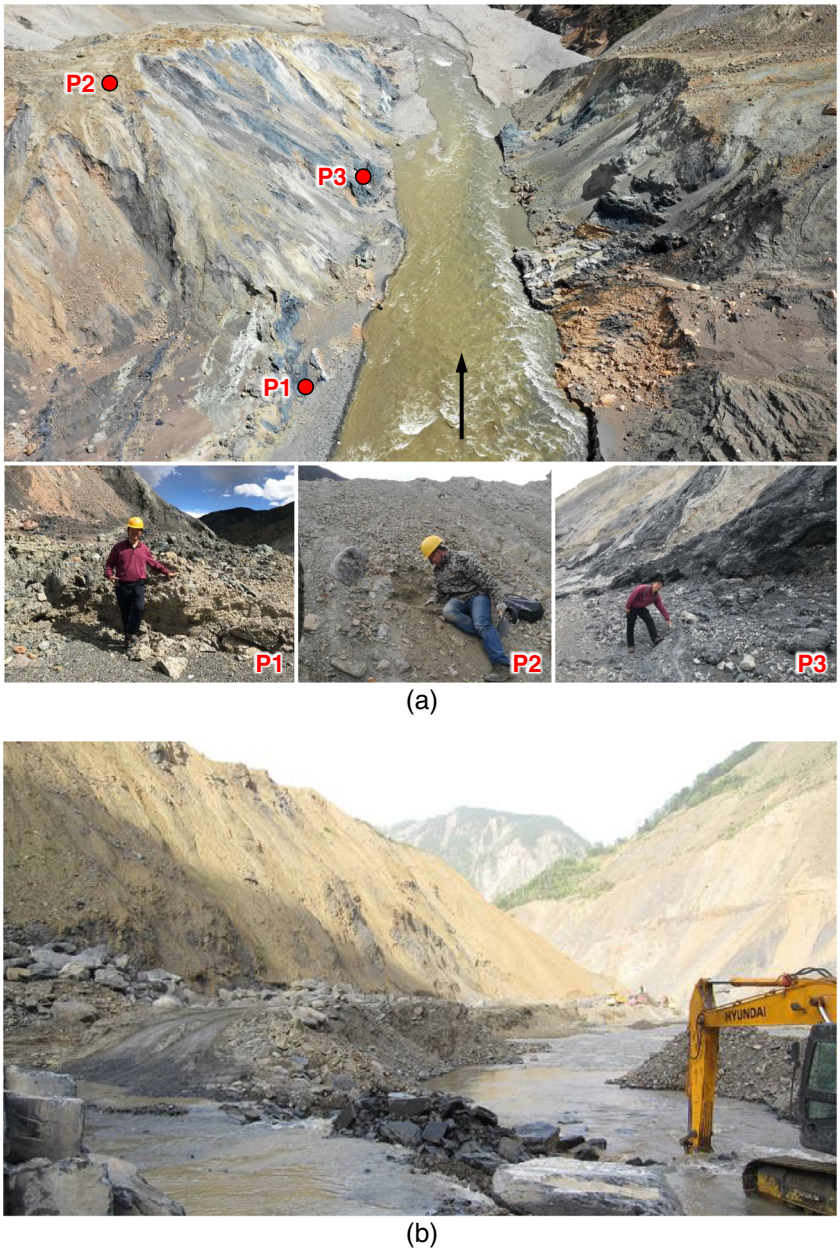

Fig. 8 Erodibility of landslide dams: **a** Baige dam featured by loose soil of medium-high erodibility at shallow depth and weathered plagioclase gneiss at the bottom; **b** Tangjiashan dam featured by top soil of medium erodibility and bottom rock mass that was not fully disintegrated (photo credit: **a**, **b** Zhang LM)

critical angle α_c. Both stages L-I and C-I are in the breach initiation phase.

(2) Stage II. The downstream of longitudinal section erodes at a constant downstream slope β_f, and the breach bottom erodes significantly in the longitudinal direction with the downstream slope eventually meeting the upstream slope (i.e., stage L-II). On the cross section (i.e., stage C-II), the breach expands both in depth and width, keeping the bank slope angle at α_c. The end of stage L-II signals the transition from the breach initiation phase to the breach development phase, while stage C-II lasts in both phases.

(3) Stage III. After the junction of the upstream and downstream slopes on the longitudinal section (i.e., stage L-III), the breach bottom erodes quickly. Hence, the flow section area increases significantly and the flow rate increases dramatically. Eventually, only vertical erosion takes place (i.e., stage C-III$_1$) on the cross section when the flow water is insufficient to cause continued bank erosion, or only horizontal erosion occurs

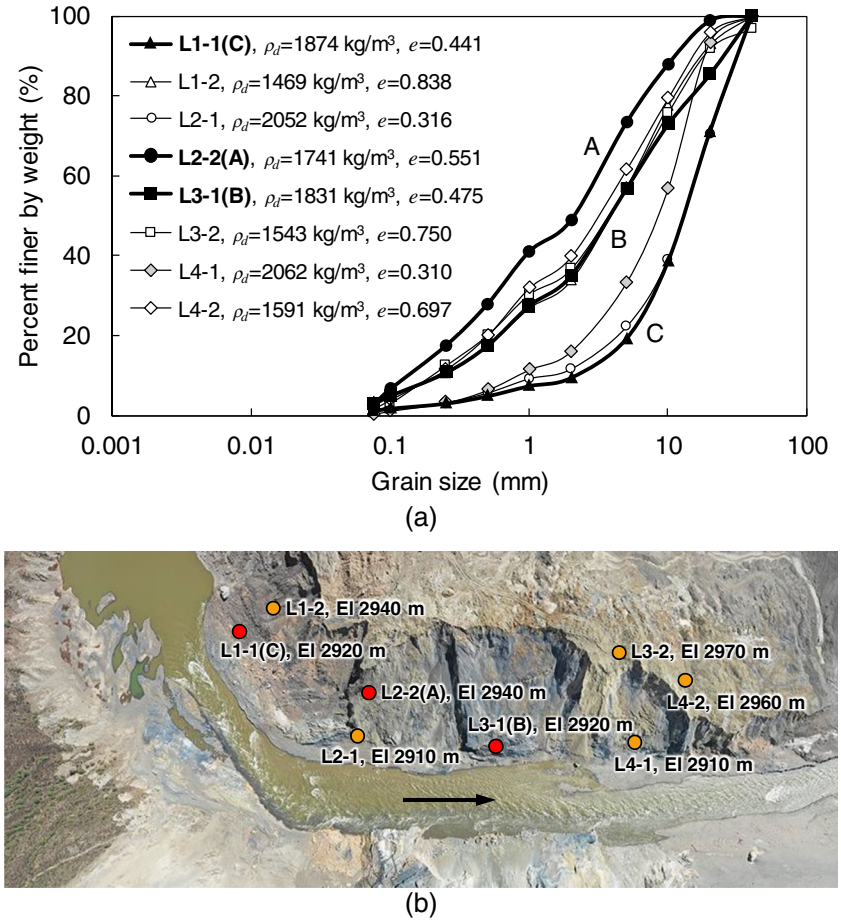

Fig. 9 Grain size distributions of the landslide deposit at indicated sampling locations: **a** grain size distribution (ρ_d = dry density, e = void ratio, and bold curves are three representatives); **b** sampling location (El = elevation)

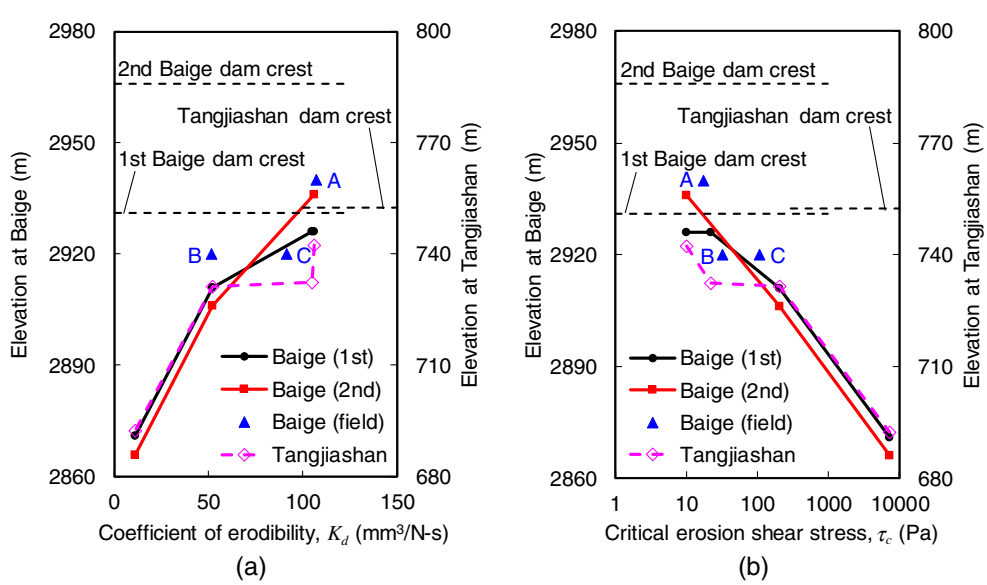

Fig. 10 Soil erodibility parameters along elevation: **a** coefficient of erodibility; **b** critical erosion shear stress

Table 1 Input parameters for empirical and numerical breaching analyses

Parameter		First dam	Second dam	Second dam without diversion channel
Basic parameter	Dam bottom elevation, D_b (m)	2870	2870	2870
	Dam crest elevation, D_t (m)	2931	2966	2966
	Dam height, H_d (m)	61	81	96
	Lake volume, V_l (m^3)	249×10^6	494×10^6	757×10^6
	Water level drop, d (m)[a]	31	51	66
	Released water volume, V_{l0} (m^3)[a]	197×10^6	442×10^6	705×10^6
	Erodibility of dam material	Medium	Medium-high	Medium-high
Hydrologic parameter	Overtopping time, T_0	17:30, 12 Oct. 2018	04:45, 12 Nov. 2018	17:10, 15 Nov. 2018
	Overtopping water level, H_w (m)	2930.1	2951.1	2965.1
	Inflow rate, Q_{in} (m^3/s)	1680	800	800
	Seepage discharge, Q_s (m^3/s)	100	0	0
Geometric parameter (cross section)	Initial breach top width, W_t (m)	5	42	5
	Initial breach bottom width, W_b (m)	2	3	2
	Initial breach depth, H_b (m)	1	15	1
	Critical breach side slope, α_c (°)	35	35	35
Geometric parameter (longitudinal section)	Initial breach bottom length, B_c (m)[b]	–	220	–
	Initial dam crest length, D_c (m)[b]	300	–	79.4
	Initial dam upstream length, L_u (m)	450	300	300
	Initial dam downstream length, L_d (m)	700	600	600
	Initial breach bottom gradient, B_g	0.006	0.006	0.006
	Critical dam downstream slope, β_f (°)	30	30	30

[a] Assume the final water level is 2900 m in the model of Walder and O'Connor (1997)

[b] Either B_c or D_c is required in DABA

(i.e., stage C-III_2) when the bed erosion is intercepted by a low erodible layer.

The required parameters in DABA for landslide dam breaching analysis are provided in Table 1, in addition to the lake capacity-elevation curve in Fig. 7b and the soil erodibility profile in Fig. 10. The geotechnical properties in Fig. 10 are the most important geotechnical inputs. The model is able to predict the outflow hydrograph, the lake water level, as well as the evolution of the breach geometry within a few minutes and can be easily implemented in spreadsheet (Peng et al. 2014) for practical applications. Such rapid prediction capability is essential to support timely decision making in mitigating risks of dam breaching flood.

Breaching of the first landslide dam

The first Baige landslide dam was overtopped naturally at 17:30, 12 October. The overflow increased dramatically at midnight, reaching a peak value of approximately 10,000 m^3/s at around 06:00 on 13 October, and returned to the base flow at 14:30 on 13 October. The maximum lake capacity during the dam breaching process was 290×10^6 m^3.

A small initial channel is assumed as shown in Table 1. The dimensions of the small initial channel will not affect the breaching progression or the final results. Figure 12a compares the hydrograph predicted by DABA and the observation reported by Cai et al. (2019), which coincide in both flow rate and time. The simulated breaching process transits from the initiation phase to the development phase at 23:59, 12 October. The predicted peak flow rate is 9706 m^3/s, occurring at 05:09, 13 October, which is slightly smaller than the observed peak flow rate of 10,000 m^3/s and slightly earlier than the observation time (i.e., 06:00, 13 October). The variation of the lake volume with time in Fig. 12a also agrees well with the observed data (CREEI 2018). The calculated total breaching duration is 25 h, including 6.5 h for initiation and 18.5 h for development, as summarized in Table 2. The simulated final breach size is also comparable with the observed one estimated on the basis of Fig. 2b. According to the evolution of the breach geometry in Fig. 13a, the final crest elevation of the residual dam is 2903.0 m. The water level decreases by 22.7 m, which is consistent with the observed value (i.e., more than 20 m) reported by media.

Table 2 Comparison of results of breaching analysis

Parameter	Method[a]	First dam	Second dam	Second dam without diversion channel
Breaching peak flow rate, Q_p (m^3/s)	Empirical equation[b] (Costa 1985) $Q_p = 0.476(H_d V_l)^{0.43}$	11,367	17,241	22,284
	Empirical equation (Costa and Schuster 1988) $Q_p = 0.0158(PE)^{0.41}$	10,221	15,204	19,419
	Empirical equation (Walder and O'Connor 1997) $Q_p = 0.99(dV_{l0})^{0.40}$	8128	13,704	18,312
	Empirical equation (Peng and Zhang 2012a) $Q_p/(g^{1/2}/H_d^{5/2}) = (H_d/H_r)^{-1.371}(V_l^{1/3}/H_d)^{1.536}e^{\alpha}$	7995	30,515	35,432
	Numerical simulation using DABA	9706	34,348	55,579
	Observation	10,000	33,900	–
Breach initiation duration, T_i (h)	Empirical equation (not available)	–	–	–
	Numerical simulation using DABA	6.5	33.4	27.9
	Observation	6.5	33.3	–
Breach development duration, T_b (h)	Empirical equation (Peng and Zhang 2012a) $T_b/T_r = (H_d/H_r)^{0.293}(V_l^{1/3}/H_d)^{0.723}e^{\alpha}$	9.2	9.0	9.3
	Numerical simulation using DABA	18.5	16.6	17.1
	Observation	14.5	17.9	–
Breach depth, H_b (m)	Empirical equation (Peng and Zhang 2012a) $H_b/H_r = (H_d/H_r)^{0.923}(V_l^{1/3}/H_d)^{0.118}e^{\alpha}$	29.9	42.2	49.2
	Numerical simulation using DABA	28.0	70.5	66.1
	Observation	32.0	61.0	–
Breach top width, W_t (m)	Empirical equation (Peng and Zhang 2012a) $W_t/H_r = (H_d/H_r)^{0.911}(V_l^{1/3}/H_d)^{0.271}e^{\alpha}$	92.3	150.3	174.2
	Numerical simulation using DABA	227.9	337.4	414.8
	Observation	180.0	300.0	–
Breach bottom width, W_b (m)	Empirical equation (Peng and Zhang 2012a) $W_b/H_d = 0.003(H_d/H_r) + 0.07(V_l^{1/3}/H_d) + \alpha$	76.2	114.2	137.9
	Numerical simulation using DABA	148.1	139.8	225.9
	Observation	80.0	90.0	–

[a] PE = potential energy, product of dam height (H_d), lake volume (V_l), and specific weight of water; d = water level drop; V_{l0} = released water volume; T_r = reference time (1 h); H_r = reference height (1.0 m); α = erodibility factor (to estimate Q_p, T_b, H_b, W_t, and W_b, α = 1.236, − 0.805, − 0.500, 0.588, and 0.624, respectively, for high erodibility; and − 0.380, − 0.674, − 0.673, 0.148, and 0.344, respectively, for medium erodibility); input parameters for empirical equations and numerical simulation are referred to Table 1

[b] Converted equation for the unit of V_l from 10^6 m^3 in the original equation to m^3

Breaching of the second landslide dam

The second landslide dam was formed on the residual of the first dam, with the lake capacity tripled. To reduce the dam-breaching risk, a 15-m depth diversion channel was completed on the afternoon of 11 November using 18 excavators and a total of 135,000 m^3 of soils/slags was excavated. Overtopped at 04:45 on 12 November, the dam experienced a 33.3-h long breach initiation phase. The outflow increased dramatically at 14:00, 13 November, and peaked at 33,900 m^3/s at 18:20, 13 November.

As shown in Fig. 12b, the hydrograph obtained by DABA agrees well with the observation data (CREEI 2018). The numerical analysis predicts a peak flow rate of 34,348 m^3/s, occurring at 19:04 on 13 November. The difference in the peak flow rate is only 1% and the time difference is less than 1 h. Figure 12b also compares the estimated lake water level at the dam site with that measured at Boluo Station 20 km upstream the dam (Fig. 7a). The simulated and observed water levels are almost identical during the first 40 h, but the simulated water level is slightly below the measured value in the final stage. This may be because the water level at Baige was almost identical to that at Boluo when the lake was full in the breach initiation phase, but was lower than that at Boluo

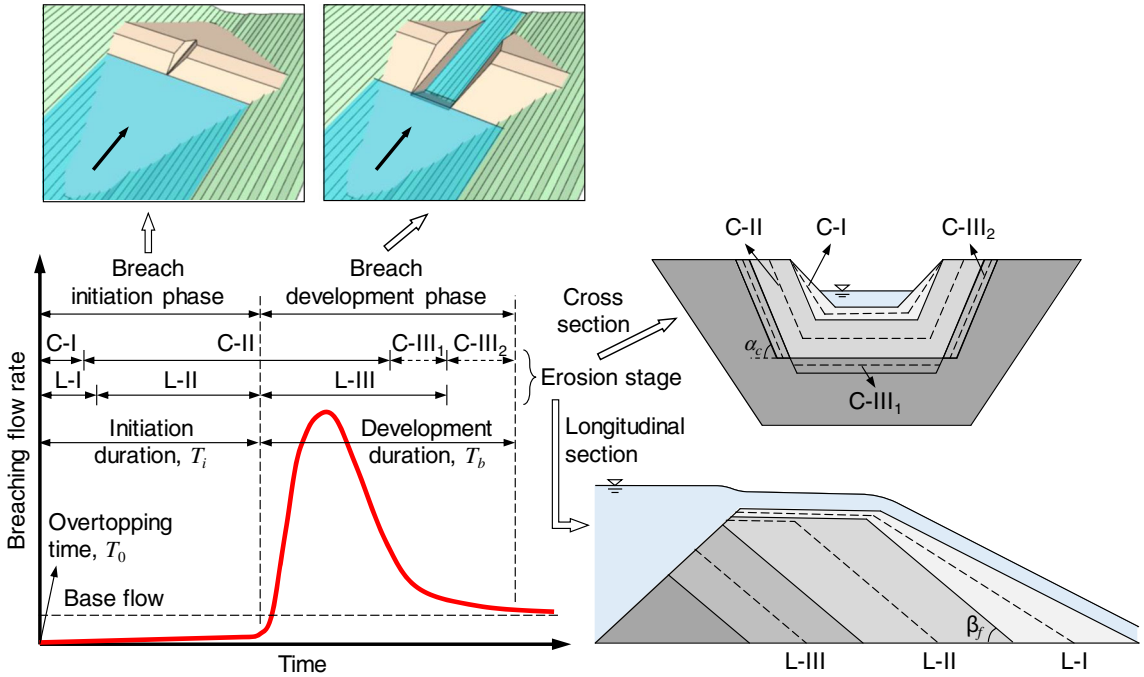

Fig. 11 Breaching process of landslide dam

during the natural flow after the completion of dam breaching (about 10 m difference in elevation).

Through field optical and unmanned aerial vehicle surveys, a 3D model of the final breach is reconstructed using photogrammetry technique, as shown in Fig. 14a. The dimensions of four cross sections of the breach are measured in Fig. 14b. The top width, bottom width and depth of the breach are in the ranges of 266–345, 77–113, and 38–94 m, respectively, and their average values are 300, 90, and 61 m as given in Table 2. The numerical simulation gives relatively accurate estimates of the breach depth and top width but slightly overestimates the bottom width. The simulated breaching progression using DABA is presented in Fig. 13b, in which the horizontal erosion terminates earlier than the vertical erosion. The final crest elevation of the residual dam is about 2895.5 m, several meters lower than the residual of the first landslide dam.

Breaching of the second landslide dam if no diversion channel were excavated

With the aid of DABA, it is possible to consider the most dangerous scenario that no diversion channel was excavated for the second landslide dam. The simulated breaching flow rate and the variation of lake water level are presented in Fig. 15. By assuming a constant inflow rate of 800 m^3/s, it would take 3.5 more days to fill the barrier lake from elevation 2951 m to elevation 2966 m, and the dam breaching would initiate at 17:10 on 15 November. Since the soil on the dam crest is more erodible, the total breaching time would be about 5 h shorter than the actual scenario with a 15-m depth diversion channel. The peak flow rate would reach 55,579 m^3/s (i.e., increased by 64%), occurring at 02:10 on 17 November, and the maximum lake water level would reach 2968.9 m, corresponding to a lake volume of 820×10^6 m^3. Obviously, the excavation of the 15-m depth diversion channel decreased the risks of the landslide dam significantly. Quantitative assessment of the landslide dam risks is beyond the scope of this paper.

Summary

The two landslide dams formed in October and November 2018 on the upper reach of the Jinsha River near Baige, Tibet, both failing by overtopping erosion, with a life span of 2.7 days for the first dam and 10.6 days for the second dam. Field investigations were conducted on the geological structure of the dam, the material properties, and the final breach dimensions. The landslide materials in the first landslide were fully disintegrated after a sufficiently long travel distance, so that the material had a medium erodibility. The second landslide was a residual landslide on the scar of the first landslide; hence, the materials forming the second landslide dam were finer and looser, having medium to high erodibility.

Both empirical equations and a physically based coupled flow-erosion numerical model, DABA, have been applied to predict the breaching parameters of the two landslide dams. Using the erodibility parameters based on the field investigations and the calibration with past landslide dams such as

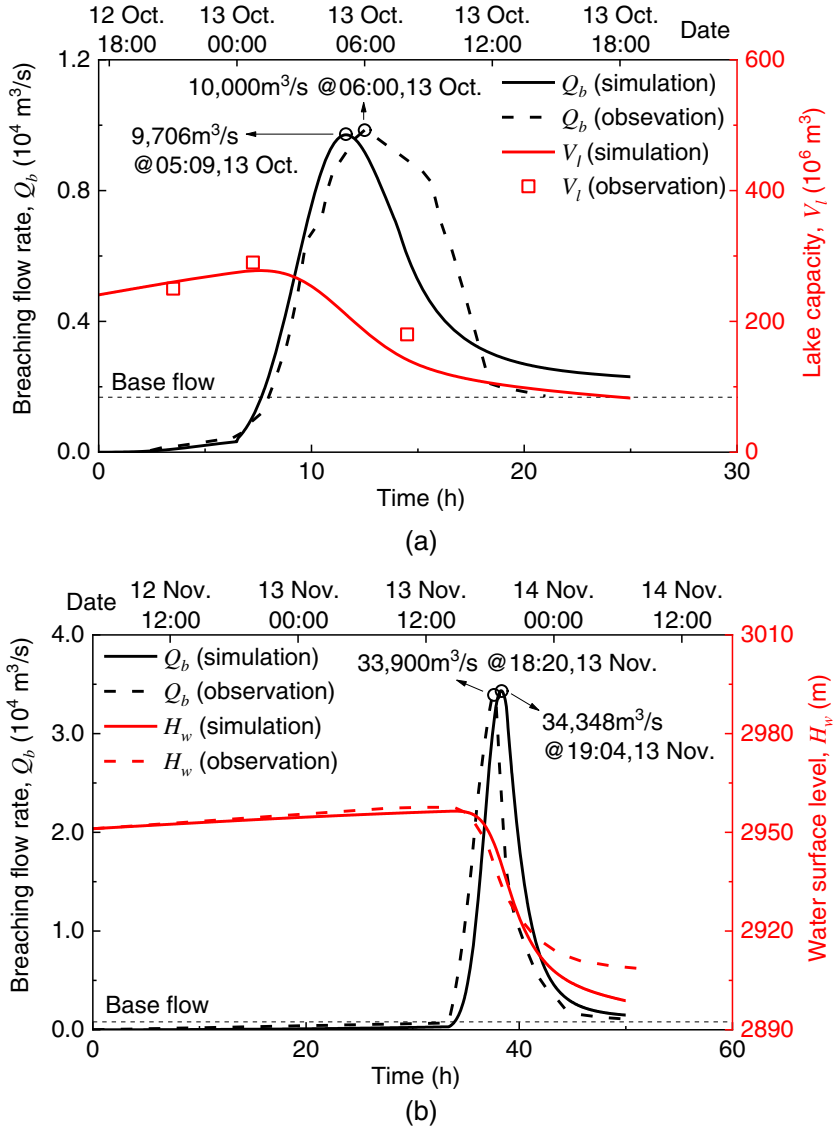

Fig. 12 Calculated results of breaching flow rate and lake water level change: **a** the first breaching on 12 October; **b** the second breaching on 12 November

Tangjiashan in 2008 and Yigong in 2000, both the empirical equations and numerical simulation provide reasonable rapid predictions for risk mitigation purposes. The peak flow rate from the empirical equations, numerical simulation, and field observation are 7995 – 11,367, 9706, and 10,000 m^3/s, respectively, for the first landslide dam and 13,704 – 30,515, 34,348, and 33,900 m^3/s, respectively, for the second landslide dam. The total breaching duration from the numerical simulation and field observation are 25 and 21 h, respectively, for the first dam and 50 and 51.2 h, respectively, for the second dam.

The construction of a diversion channel on the crest of the second landslide dam is proven to be a very effective measure for reducing the peak flow rate. If no channel had been constructed, the peak flow rate would have reached 55,579 m^3/s in the numerical simulation.

More detailed field geological investigations and laboratory characterization of the damming materials have to be performed in the future to better characterize the internal structure and simulate the erosion process of the landslide dams.

Acknowledgments

This research is coordinated by Prof. Yaojun Cai of Changjiang Institute of Survey, Planning, Design and Research, Changjiang Water Resources Committee. Part of the information in this paper is from news released by government agencies and media.

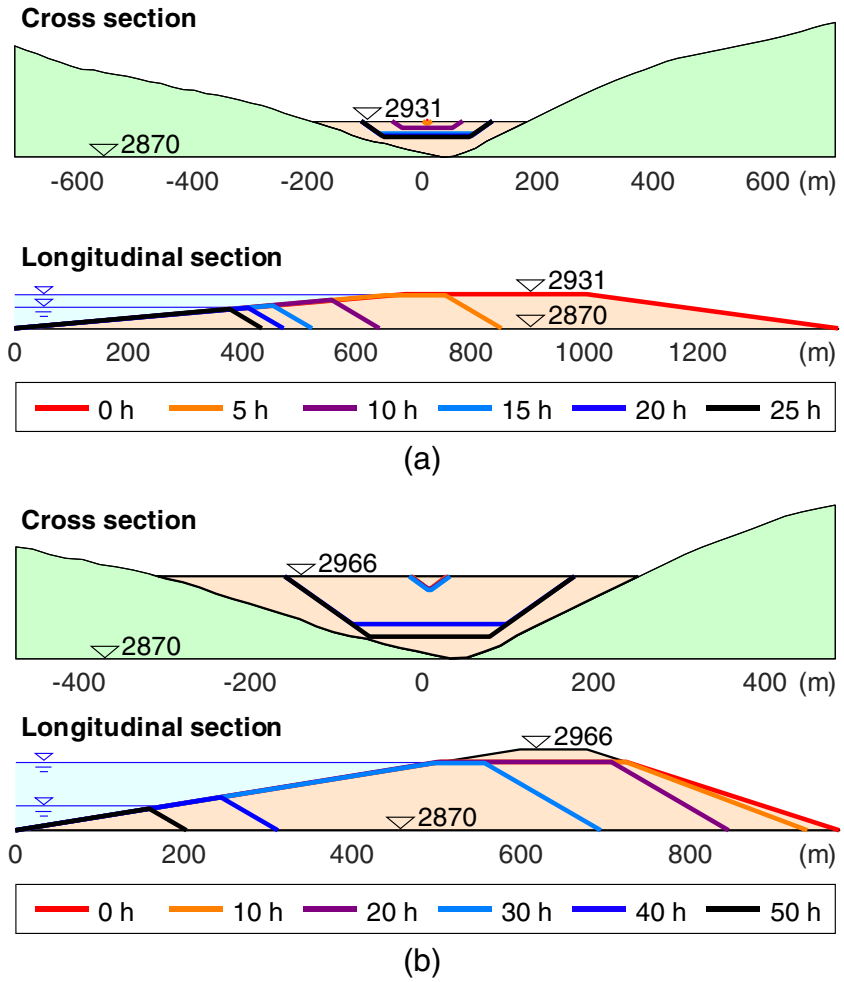

Fig. 13 Computed breach evolution with time: **a** the first breaching on 12 October; **b** the second breaching on 12 November

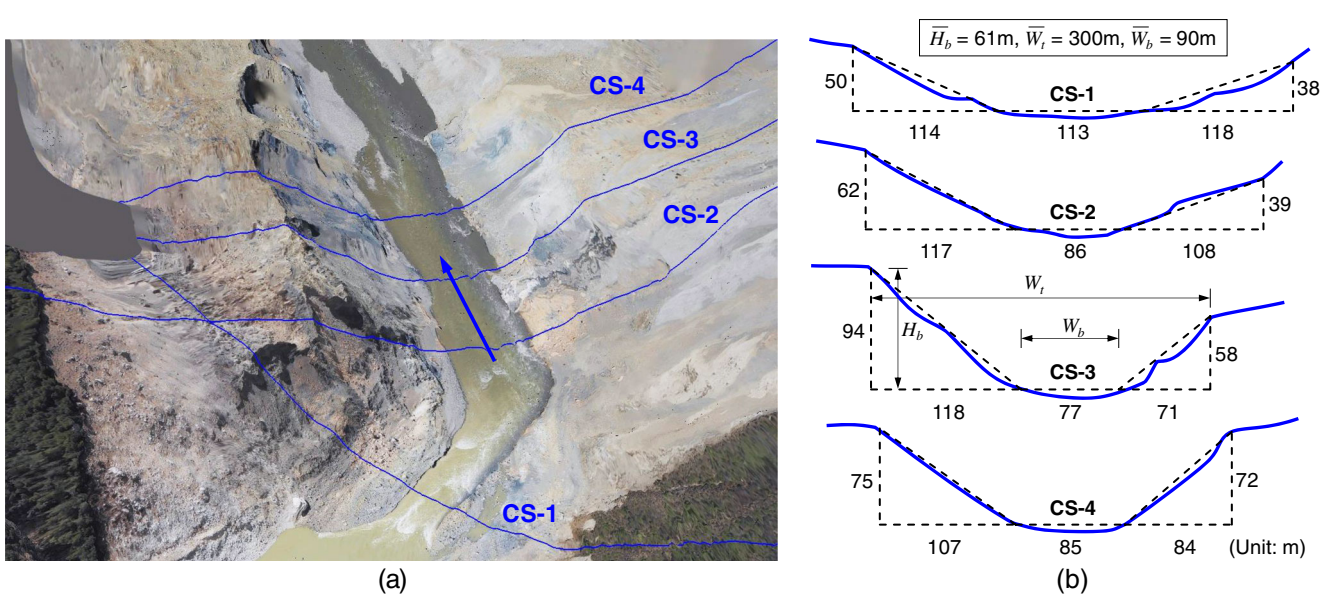

Fig. 14 Observed final breach dimensions: **a** selected cross sections in 3D model; **b** estimated breach size

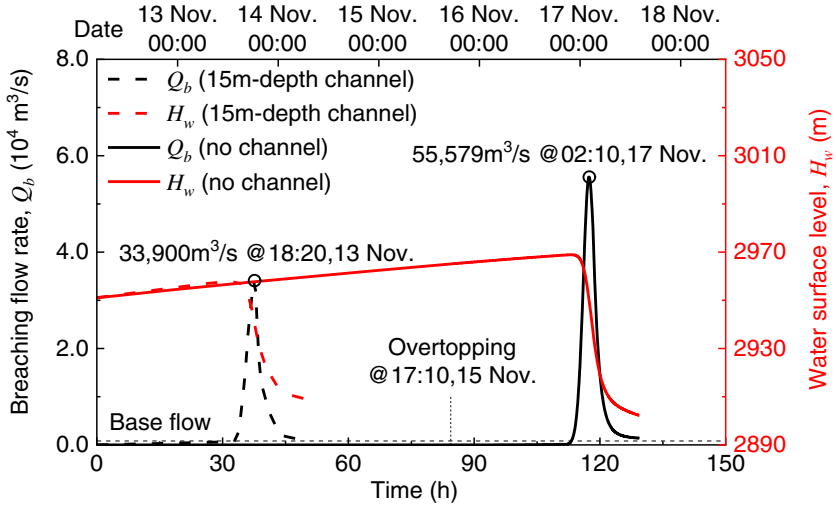

Fig. 15 Numerical simulation of the second dam breaching without diversion channel

Funding information

Financial support was from the National Key Research and Development Program of the Ministry of Science and Technology of China (Project No. 2018YFC1508600).

References

Annandale GW (2006) Scour technology - mechanics and engineering practice. McGraw-Hill, New York

Briaud JL (2008) Case histories in soil and rock erosion: Woodrow Wilson bridge, Brazos River meander, Normandy cliffs, and New Orleans levees. J Geotech Geoenviron Eng 134(10):1425–1447

Cai YJ, Luan YS, Yang QG, Xu FX, Zhang SJ, Shi Y, Yi DLZ (2019) Study on structural morphology and dam - break characteristics of Baige barrier dam on Jinsha River. Yangtze River 50(3):15–22 (in Chinese)

Chang DS, Zhang LM (2010) Simulation of the erosion process of landslide dams due to overtopping considering variations in soil erodibility along depth. Nat Hazards Earth Syst Sci 10(4):933–946

Chang DS, Zhang LM, Xu Y, Huang RQ (2011) Field testing of erodibility of two landslide dams triggered by the 12 May Wenchuan earthquake. Landslides 8(3):321–332

Chen S, Chen Z, Tao R, Yu S, Xu W, Zhou X, Zhou Z (2018) Emergency response and back analysis of the failures of earthquake triggered cascade landslide dams on the Mianyuan River, China. Nat Hazards Rev 19(3):05018005

Chen Z, Ma L, Yu S, Chen S, Zhou X, Sun P, Li X (2015) Back analysis of the draining process of the Tangjiashan barrier lake. J Hydraul Eng 141(4):05014011

China Renewable Energy Engineering Institute (CREEI) (2018) Report on emergency disposal of Baige landslide dams, Jinsha River. Beijing, China (in Chinese)

Costa JE (1985) Floods from dam failures. U.S. Geological Survey, Open-File Report 85–560

Costa JE, Schuster RL (1988) The formation and failure of natural dams. Geol Soc Am Bull 100:1054–1068

Cui P, Dang C, Zhuang JQ, You Y, Chen XQ, Scott KM (2012) Landslide-dammed lake at Tangjiashan, Sichuan province, China (triggered by the Wenchuan earthquake, May 12, 2008): risk assessment, mitigation strategy, and lessons learned. Environ Earth Sci 65(4):1055–1065

Danka J, Zhang LM (2015) Dike failure mechanisms and breaching parameters. J Geotech Geoenviron Eng 141(9):04015039

Dong JJ, Lai PJ, Chang CP, Yang SH, Yeh KC, Liao JJ, Pan YW (2014) Deriving landslide dam geometry from remote sensing images for the rapid assessment of critical parameters related to dam-breach hazards. Landslides 11(1):93–105

Fan X, Xu Q, Alonso-Rodriguez A, Subramanian SS, Li W, Zheng G, Dong X, Huang R (2019) Successive landsliding and damming of the Jinsha River in eastern Tibet, China: prime investigation, early warning, and emergency response. Landslides 16(5):1003–1020

Hanson GJ, Simon A (2001) Erodibility of cohesive streambeds in the loess area of the midwestern USA. Hydrol Process 15(1):23–38

Ouyang CJ, An HC, Zhou S, Wang ZG, Su PC, Wang DP, Cheng DX, She JX (2019) Insights from the failure and dynamic characteristics of two sequential landslides at Baige village along the Jinsha River. China Landslides 16(7):1397–1414

Peng M, Zhang LM (2012a) Breaching parameters of landslide dams. Landslides 9(1):13–31

Peng M, Zhang LM (2012b) Analysis of human risks due to dam break floods - part 1: a new model based on Bayesian networks. Nat Hazards 64(1):903–933

Peng M, Zhang LM (2012c) Analysis of human risks due to dam break floods - part 2: application to Tangjiashan landslide dam failure. Nat Hazards 64(2):1899–1923

Peng M, Zhang LM (2013a) Dynamic decision making for dam-break emergency management - part 1: theoretical framework. Nat Hazards Earth Syst Sci 13:425–437

Peng M, Zhang LM (2013b) Dynamic decision making for dam-break emergency management - part 2: application to Tangjiashan landslide dam failure. Nat Hazards Earth Syst Sci 13:439–454

Peng M, Zhang LM, Chang DS, Shi ZM (2014) Engineering risk mitigation measures for the landslide dams induced by the 2008 Wenchuan earthquake. Eng Geol 180:68–84

Shi ZM, Xiong X, Peng M, Zhang LM, Xiong YF, Chen HX, Zhu Y (2017) Risk assessment and mitigation for the Hongshiyan landslide dam triggered by the 2014 Ludian earthquake in Yunnan, China. Landslides 14(1):269–285

Singh VP, Scarlatos PD (1988) Analysis of gradual earth-dam failure. J Hydraul Eng 114(1):21–42

Tadono T, Ishida H, Oda F, Naito S, Minakawa K, Iwamoto H (2014) Precise global DEM generation by ALOS PRISM. ISPRS Ann Photogr Remote Sens Spatial Inform Sci II-4:71–76

Tibet Autonomous Region Geological Surveys (TARGS) (1992) China regional geological survey report & regional geology map – Baiyu, Report No. H-47-09. Lhasa, China (in Chinese)

Walder JS, O'Connor JE (1997) Methods for predicting peak discharge of floods caused by failure of natural and constructed earthen dams. Water Resour Res 33(10):2337–2348

Zhang LM, Peng M, Chang DS, Xu Y (2016) Dam failure mechanisms and risk assessment. John Wiley & Sons, Singapore

Zhang LM, Xu Y, Huang RQ, Chang DS (2011) Particle flow and segregation in a giant landslide event triggered by the 2008 Wenchuan earthquake, Sichuan, China. Nat Hazards Earth Syst Sci 11:1153–1162

Zhang Z, He SM, Liu W, Liang H, Yan SX, Deng Y, Bai XQ, Chen Z (2019) Source characteristics and dynamics of the October 2018 Baige landslide revealed by broadband seismograms. Landslides 16(4):777–785

Zhou JW, Cui P, Hao MH (2016) Comprehensive analyses of the initiation and entrainment processes of the 2000 Yigong catastrophic landslide in Tibet, China. Landslides 13(1):39–54

Zhu H, Zhang LM (2016) Field investigation of erosion resistance of common grass species for soil-bioengineering in Hong Kong. Acta Geotech 11(5):1047–1059

L. Zhang · T. Xiao · J. He · C. Chen
Department of Civil and Environmental Engineering,
The Hong Kong University of Science and Technology,
Hong Kong, China

T. Xiao
e-mail: xiaote@ust.hk

J. He
e-mail: jhebl@connect.ust.hk

C. Chen
e-mail: laurachen@ust.hk

L. Zhang · C. Chen
State Key Laboratory of Hydraulics and Mountain River Engineering, College of Water Resource and Hydropower,
Sichuan University,
Chengdu, China

L. Zhang (✉)
HKUST Shenzhen Research Institute,
Shenzhen, China
Email: cezhangl@ust.hk